Journal of Materials Chemistry

Cite this: J. Mater. Chem., 2012, 22, 13903

www.rsc.org/materials

COMMUNICATION

Robust plasmonic sensors based on hybrid nanostructures with facile tunability†

Chul-Joon Heo,[a] Hwan Chul Jeon,[a] Su Yeon Lee,[a] Se Gyu Jang,[a] Soojeong Cho,[a] Yeonho Choi*[b] and Seung-Man Yang*[a]

Received 29th March 2012, Accepted 21st May 2012
DOI: 10.1039/c2jm31958f

Here, we demonstrate the preparation of a hybrid nanoplasmonic probe array, a nanoforest, which consists of gold nanostructures coated on top of silica nanospheres and evaporated gold film structure onto bottom through masks. Optically tunable plasmonic surfaces could be achieved by varying the nanoforest fabrication conditions, which acted as a selective nanoantenna. Plasmon coupling effects were effectively controlled by adjusting the vertical distance (nanogap) between the gold nanostructures on the silica bead and the bottom. Such control is critical to highly sensitive molecular detection applications. As a proof of concept, nanoforests were used as colorimetric sensors of refractive index changes. The sensors were highly sensitive and displayed distinct colors for small refractive index (RI) changes. The flexible and sensitive near/far-field optical properties render these nanoforests excellent plasmonic substrates for quantitative, sensitive and label-free sensing with nanoscale spatial resolution.

The extraordinary optical properties of metallic nanostructures on the subwavelength scale, which arise from interactions between light and surface plasmons, have attracted interest for their use in photonic, plasmonic, chemical/biological nanosensor applications and nanoscale electronics.[1–4] Because the optical properties can be manipulated by changing the shape, size, and composition of the nanostructures, control over these parameters on the 10–100 nm length scale provides a means for increasing the sensitivity and selectivity of plasmonic-based molecular detection methods, including localized surface plasmon resonance (LSPR),[5–7] surface enhanced Raman spectroscopy (SERS),[8–10] and plasmon resonance energy transfer (PRET).[11,12] Lithographic applications may be performed *via* two general modes: parallel processing or serial writing. Although parallel processing modes, such as photolithography and nanoimprinting techniques, are useful for cost-effective, high-throughput, and large-area patterning, these methods can only duplicate predefined patterns and the manipulation of nanostructure designs to create a selective nanoantenna is limited.[13–15] Serial writing methods, including electron beam lithography (EBL) and focused ion-beam lithography (FIB), provide limited throughput, although they can achieve high spatial resolution and permit greater flexibility in the design of a material.[16] However, uniform and precisely controlled nanoplasmonic probe arrays are essential for quantitative, sensitive, and selective molecular identification with high spatial resolution.[17,18]

Here, we propose a simple and robust method for preparing hybrid nanoplasmonic arrays with high throughput. Nanoforests, which are arrays of hexagonally arranged gold nanostructures, were prepared by directional deposition on tree-shaped SiO_2/PS (polystyrene) composite masks *via* colloidal lithography. Colloidal lithography is a versatile nanofabrication method that uses self-organized colloids as a template or mask.[19,20] Colloidal lithography provides an easy method for fabricating nanoscale features in a regular and reproducible manner, and it permits formation of novel shapes molded from spheres. In this manner, colloidal lithography can be an attractive method for preparing plasmonic substrates. A reproducible and robust lithographic technique was pioneered by the Van Duyne group to fabricate an Au film over nanospheres (FON) or nanoparticle arrays for novel plasmonic substrates.[5] As we shall see shortly, for our nanoforest, the vertical feature size can be freely controlled, which gives an additional degree of freedom in tuning plasmonic responses compared with the FON or nanoparticle arrays. As shown in Fig. 1a–c, hybrid plasmonic antenna arrays were composed of gold half shells deposited on tree-shaped masks with nanohole arrays formed on a substrate. The hybrid plasmonic substrates introduced here exhibited coupled surface plasmons (SP) in the visible range, and their optical properties could be tuned precisely by varying the structural parameters. The plasmonic properties depended strongly on the shape and size of nanostructures. Furthermore, the vertical nanogap between plasmonic structures could be controlled, resulting in a large electromagnetic (EM) field enhancement due to the gap. Uniform EM field enhancements in nanoforests are expected to be useful in plasmonic nano-imaging and the spatial analysis of system as well as in SERS measurements. Ordered gold nanoforests exhibited vivid colored reflections under white light illumination. The reflected light depended on both the wavelength of the resonant extinction and on the shape of the extinction spectrum. The plasmonic extinction could be precisely

[a]National CRI Center for Integrated Optofluidic Systems, Department of Chemical and Biomolecular Engineering, KAIST, Daejeon, 305-701, Korea. E-mail: smyang@kaist.ac.kr; Fax: +82 42-350-5962
[b]Department of Biomedical Engineering, Korea University, Seoul, 136-703, Korea. E-mail: yeonhochoi@korea.ac.kr
† Electronic supplementary information (ESI) available. See DOI: 10.1039/c2jm31958f

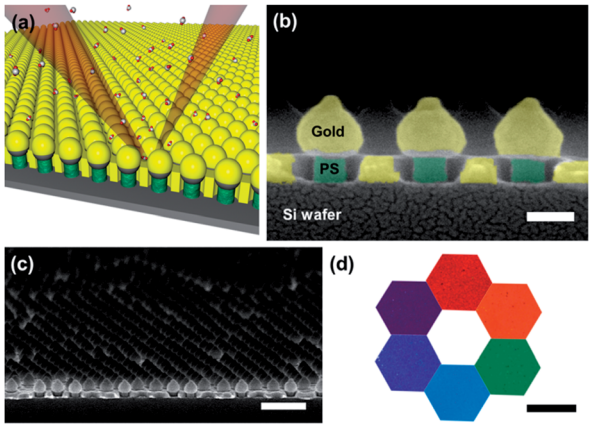

Fig. 1 Nanoforest with a nanogap array. (a) Schematic diagram of uniformly arranged nanogaps for plasmonic detection of target molecules with nanometer-scale resolution. (b) Cross-sectional SEM image of a nanoforest with false colors (yellow for gold, green for PS), scale bar is 100 nm. (c) Scanning electron microscopy (SEM) image of a plasmonic nanoforest over a large area, the scale bar is 1 μm. (d) Palette of reflected colors from plasmonic substrates containing various nanoforest arrays on the surface, the scale bar is 50 μm. Corresponding structural parameters of each of the reflection color images were identified with the following format (D_g, τ, H_g); red (144 nm, 60 nm, 72 nm), orange (139 nm, 40 nm, 67 nm), green (175 nm, 40 nm, 50 nm) under ethanol (n = 1.36), sky blue (178 nm, 20 nm, 85 nm), dark blue (180 nm, 20 nm, 68 nm), purple (182 nm, 20 nm, 59 nm).

controlled *via* refractive index (RI, n) changes by applying solvents with various refractive indices over the visible range.

Gold nanoforests were fabricated using colloidal lithography.‡ Fig. S1† shows a schematic description of the fabrication of plasmonic nanoforest structures. (1) First, a PS solution was spin-coated onto a silicon substrate to form a PS thin film. Monodispersed silica nanospheres self-organized on the oxygen plasma-treated PS thin film during spin-casting. By optimizing the concentration of the silica particles in ethanol and the spin speed, spin-casting of the silica spheres could be optimized to form a crystalline single layer. (2) Assembled silica spheres were embedded into the PS film by annealing the substrate above the glass transition temperature (T_g). Under certain conditions (temperature = 110 °C and embedding time = 2 min), silica particles equilibrated to positions in which a balance was reached between the force of the polymer viscosity, which drove embedding, and the surface tension, which opposed embedding.[10] After embedding the silica particles into the PS film, silica particles remained in position during the following etching steps. (3) To prepare the mask for metal deposition, silica particles and the PS film were treated to a two-step dry etching procedure: CF_4 reactive ion etching (RIE) reduced the silica particle size, and O_2 RIE defined the polymeric poles to support the silica particles. (4) The resulting tree-shaped composite masks were submitted to highly directional deposition of gold by e-beam evaporation. During gold deposition, the silica–PS composite masks blocked deposition of metal beneath the mask. After deposition of a thin gold film, a gold nanoforest composed of two different metal nanostructures was prepared: gold nanohole arrays and gold-deposited nanotree arrays. Because the method of fabricating the nanoforests began from well-ordered silica nanosphere arrays, both nanostructured plasmonic arrays showed a hexagonal arrangement over large areas.

Fig. 1a shows a schematic description of the biomolecular sensing process using a uniform plasmonic nanoforest. A regularly ordered plasmonic array provides "hot spots" for SERS characterization due to the presence of highly enhanced electromagnetic (EM) fields as a result of the small feature size. The feature size was easily tuned from several nanometers to hundreds of nanometers by varying the mask design and deposition thickness. Fig. S2† lists several parameters that contributed to the morphologies of the tree-shaped mask and the gold nanoforest. Two important size parameters characterized the structure of a tree-shaped composite mask, and these parameters determined the gold nanoforest: the bottom-to-silica diameter length (H_s), and the sculptured silica diameter (D_s). After depositing a gold thin film on the composite mask, the bottom-to-gold deposited on silica (H_g) and the diameter of the gold spheres deposited silica diameter (D_g), which is deviated from H_s and D_s to an extent that depended on the deposition thickness (τ), directly influenced the optical characteristics of the nanoforest. Three structural parameters, H_g, D_g and τ were used to describe the geometrical dependence of plasmonic properties of the nanoforests. Small differences in these parameters affected the optical properties of the metal nanostructures.[21] A cross-sectional scanning electron microscopy (SEM) image with false colors (yellow for gold, green for PS) of a representative gold nanoforest with H_g = 68 nm, D_g = 144 nm and τ = 60 nm is presented in Fig. 1b. Uniformly ordered gold nanoforests over a large area were prepared by colloidal lithography, as described above (Fig. 1c). Because the ordered nanoforests were characterized by extinction bands in the visible region, substrates containing nanoforest structures exhibited vivid color reflection. A palette of colors reflected from nanoforest substrates, recorded using optical microscopy (OM) images of nanoforests, is presented in Fig. 1d. These images show that most colors, from purple to red, could be reflected by the nanoforest substrates.

The plasmonic properties of the metal nanostructures could be tuned by varying the feature size at a given geometry. Several methods may be used to change the structural features of the 3D hybrid metal nanostructures. Three approaches were tested for their ability to tune the optical properties of the gold nanoforests: (1 and 2) the vertical feature size was varied by varying H_g and τ, or (3) the lateral size of the structure was varied by varying D_g. These approaches were tested by varying one fabrication condition so as to vary the target feature size without affecting the other structural parameters. To control the vertical geometry of the nanoforests, the height of PS pillars or the deposition depth of the gold could be changed. The properties of the nanoforests could also be tuned by varying the lateral size of the structures by changing the diameter of the gold-deposited silica mask.

As a first approach for controlling the nanoforest feature size, τ was varied without changing the design of the deposition mask. By increasing the quantity of gold deposited onto the tree-like composite structures with a given feature size, nanoforest structures with smaller nanogaps were fabricated. For this approach, H_g of the target mask should be smaller than the gold layer thickness. Here, three deposition conditions (20, 40, 60 nm) were tested on nanotree arrays with D_s = 160 nm and H_s = 70 nm. The insets in the upper left region of Fig. 2a–c show schematic descriptions of this approach. Gold nanoforests fabricated with thicker gold deposition layers yielded a smaller distance between the plasmonic structures (Fig. 2a–c). The size of the gold-deposited silica nanospheres also increased as the deposition layer thickness increased. However, the lateral size variance was not

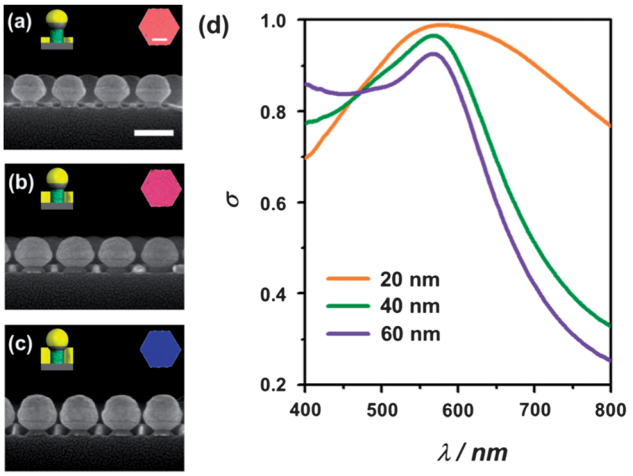

Fig. 2 Tuning of the vertical size by varying the amount of gold deposition. (a–c) Cross-sectional SEM images of gold nanoforests with different deposition depths. τ values for structures are 20, 40 and 60 nm, respectively. Insets are optical microscopy images of reflected colors from a plasmonic substrate containing gold nanoforests. Scale bars are 200 nm. Scale bars in insets are 20 μm. (d) Extinction spectra of nanoforests with different τ values corresponding to structures of (a–c) (orange: a, 20 nm, green: b, 40 nm, purple: c, 60 nm).

large, and the effects on the plasmonic properties were insignificant compared with vertical size difference. The nanoforest structure feature sizes were measured from SEM images, as shown in Fig. 2. Gold deposition layers with 20 nm thick produced nanoforests with $D_g = 175$ nm, $H_g = 60$ nm. Gold deposition of 40 nm and 60 nm thick produced nanoforest structural parameters of $D_g = 185$ nm, $H_g = 63$ nm for the 40 nm gold film, and $D_g = 190$ nm, $H_g = 66$ nm for the 60 nm gold film. The plasmonic properties of the nanoforests were characterized by measuring the reflectance spectra under normal incidence conditions. The plasmonic extinction of the nanoforest was evaluated by subtracting the reflectance R from unity, $\sigma = 1 - R$ considering highly reflective plasmonic substrates consisting mainly of gold nanomaterials and silicon substrates. Fig. 2d shows the extinction spectra of three gold nanoforests with different values of τ. As the deposition depth was increased from 20 to 60 nm, the width of the plasmonic peak narrowed while the resonant wavelength (λ_p) remained constant at 570 nm. The resonant wavelengths of nanoforests prepared with 20 nm, 40 nm and 60 nm thick gold films were 575 nm, 567 nm and 566 nm, respectively. The insets in the upper right regions of each of the SEM images (Fig. 2a–c) show the reflected colors from plasmonic substrates consisting of gold nanoforests with certain surface geometries. The reflection color, which depended on the plasmonic properties, could be varied by controlling the amount of gold deposited on the mask. The reflection colors of three nanoforest substrates could be explained by analyzing the shapes of the extinction spectra. The color reflected from a structured plasmonic substrate depends on the optical response to incident light in the visible range ($\lambda = 400$–700 nm). As the width of the plasmonic peak decreased, the color of the plasmonic substrate changed from bright pink to dark pink, then to dark blue. A nanoforest substrate with a 60 nm nanogap produced a broad dip in the extinction spectrum over the range of 400–500 nm, which resulted in a bluish substrate color.

The vertical geometry could also be controlled by tuning the vertical size parameters of the mask. Under fixed deposition conditions (40 nm), H_g was varied by controlling the height of the PS pillars that supports silica spheres. For fixed dry etching conditions, only the initial thickness of the PS affected H_g of the resulting nanoforest structure. The thickness of the PS thin film was varied by changing the concentration of the PS solution in toluene (0.5–1.5 wt%) and the spin-coating rotational speed (1000–4000 rpm). Three nanoforest structures were prepared, and the morphologies and optical properties were characterized as described above (Fig. S3†). Nanoforests fabricated from 45 nm, 80 nm and 150 nm thick PS films yielded H_g values of 48 nm, 63 nm and 81 nm, respectively (Fig. S3a–c†). D_g was held constant at ~185 nm by fixing the conditions under which the silica particles were etched. As shown in Fig. S3d†, the extinction characteristics of the nanoforests were investigated by measuring the reflectivity over the visible range. In contrast to previous results, λ_p for the nanostructures gradually shifted to longer wavelengths from 559 nm to 567 nm and 584 nm, as H_g increased. The reflection colors of the nanoforest substrates varied depending on the optical properties of the structures. The nanoforest with $H_g = 81$ nm showed a broad dip at ~420 nm, which gave rise to a purple color.

In addition to varying the vertical dimensions of the nanoforests, the lateral dimensions were varied in an effort to tune the plasmonic properties. The optical properties of a plasmonic material depend on the lateral feature size, as reported in studies of a variety of plasmonic structures.[21] Nanoforest arrays were fabricated with various deposition masks for varying silica etching times, 90–150 s. Increasing the CF_4 RIE time decreased the diameter of silica spheres (D_s) in the mask. SEM images and extinction spectra of three nanoforests with different D_g values are shown in Fig. 3, along with their OM images showing the reflected colors. As expected, a longer silica etching time produced nanoforests with smaller D_g and a smaller hole diameter. At RIE times of 90 s, 120 s and 150 s CF_4 RIE, nanoforests with D_g values of 190 nm, 176 nm and 144 nm were prepared, as shown in Fig. 3a–c. The optical properties of these structures indicated that the resonant wavelength (λ_p) shifted to shorter wavelengths, from 556 nm (Fig. 3a) to 552 nm

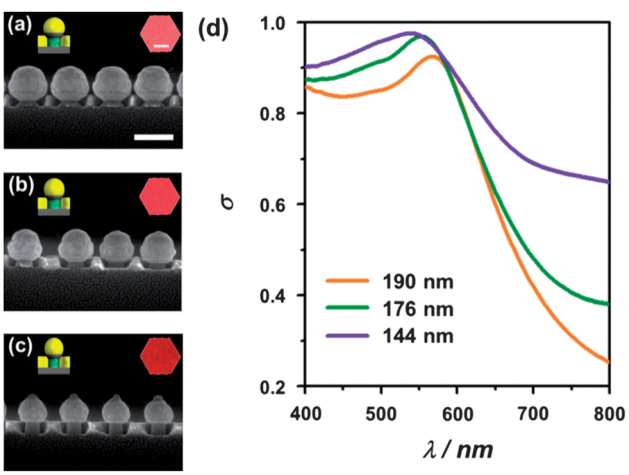

Fig. 3 Tuning of the lateral size of the nanoforest by varying the size of the mask for deposition. (a–c) SEM images of gold nanoforests with different values of D_g. Resulting D_g values are 190, 176 and 144 nm, respectively while the nanogap size was kept constant. Insets are optical microscopy images of reflected colors from plasmonic substrates. Scale bars are 200 nm. Scale bars in insets are 20 μm. (d) Plasmonic properties of nanoforests with different D_g values corresponding to structures of (a–c) (orange: a, green: b, purple: c).

(Fig. 3b) and 538 nm (Fig. 3c). As D_g decreased, the extinction of the nanoforest substrates increased over the visible range and the extinction spectrum shifted toward the blue as shown in Fig. 3d. Changes in the extinction spectrum were achieved by tuning the lateral dimensions of the nanoforest. The reflected colors changed from bright pink to red. By combining the three approaches for controlling the plasmonic properties of nanoforests (two methods for varying the vertical dimensions and one method for varying the lateral dimension), several types of nanoforests could be fabricated. The tunable resonance range was narrow compared with other plasmonic substrates, but materialization of most of the reflected color was achievable with nanoforest structures by controlling the various structural parameters. As described above, the plasmonic substrate colors depended mainly on the shape and λ_p of the extinction spectra, which were tuned by varying several feature size parameters.

The optical properties of plasmonic materials are highly sensitive to small changes in the surrounding environment.[5,22] The response of plasmonic properties to refractive index (RI, n) changes was explored by introducing solvents with different refractive indices to the nanoforest substrates, including methanol ($n = 1.33$), ethanol ($n = 1.36$), 2-propanol ($n = 1.38$), silicon oil ($n = 1.41$), hexadecane ($n = 1.44$), toluene ($n = 1.50$), and 1,2,4-trichlorobenzene ($n = 1.57$). After applying solvents to the plasmonic substrate, the altered reflection colors were recorded by collecting OM images from the nanoforests and the corresponding extinction spectra were measured. Two representative nanoforest substrates with similar resonant wavelengths (λ_p) and different geometries were selected for testing the RI response. Nanoforests having $D_g = 175$ nm, $\tau = 40$ nm and $H_g = 50$ nm originally exhibit a resonance at 568 nm in the dried state and a bright pink reflection color (Fig. 4a and c). The surrounding RI was increased by applying solvents of higher RI. The color reflected from the substrate changed first to green, then to yellowish green. This phenomenon could be explained by analyzing the extinction spectra collected in the presence of the different solvents (Fig. 4c). The extinction spectrum in the dried state shifted gradually to longer wavelengths due to a higher surrounding RI. The spectral red-shift was accompanied by a shift in the broad dip from the original position at ultraviolet (UV) region which also shifted to visible range (~550 nm). This shift produced a green reflected color. Further increases in the RI forced the reflectivity (R) around 600 nm to increase, and the color changed from green to a yellowish green. Fig. 4b shows the optical response to changes in the RI on a nanoforest with $D_g = 139$ nm, $\tau = 40$ nm and $H_g = 80$ nm. The nanoforest shown in Fig. 4 displayed extinction at 561 nm and a dark pink reflection color. The surrounding RI increased upon application of a solvent with a higher RI, which shifted the reflection color from bright purple to sky blue as shown in Fig. 4b. During the spectral red-shift, a broad dip appeared at ~400 nm, which shifted the purple reflection to ~500 nm and produced a blue reflected color. For both cases, the λ_p values in the dried state were almost identical for a given nanoforest structure. However, the sensitivities to refractive index changes and the optical responses in the UV region differed significantly. These differences were observed in the spectral shifts induced by increasing the surrounding RI. The bulk sensitivity was quantitated by measuring the resonance wavelength differences as a function of the refractive index change ($\delta\lambda_p/\delta n$). The nanoforests shown in Fig. 4a and c showed higher bulk sensitivities (183.6 nm per RIU) than did the nanostructure shown in Fig. 4b and S4† (81.4 nm per RIU). These results suggest that both the plasmonic properties and the sensitivity to RI changes depended strongly on the shape and size of the plasmonic structure. Clear differences in the reflection color as a function of RI were observed in the nanoforest substrates, indicating that molecular recognition based on RI changes may be possible with nanoforest substrates.

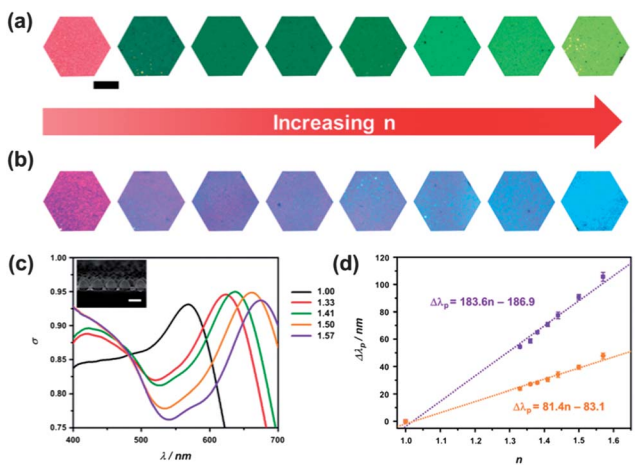

Fig. 4 Optical response of nanoforest to refractive index (n) change. (a–b) Change of reflection colors from representative plasmonic substrates when solvents with different n values were applied. (c) Extinction spectra of nanoforests under various solvents (1.00: air, 1.33: ethanol, 1.44: hexadecane, 1.50: toluene, 1.57: 1,2,4-trichlorobenzene). Inset shows the cross-sectional SEM image of a gold nanoforest. The scale bar is 200 nm. (d) Variation of resonant wavelength ($\Delta\lambda_p$) with respect to refractive index change.

The gold nanoforests were tested as molecular sensors in the context of SERS detection of adsorbed molecules. The nanoforest described in Fig. 1b was used for molecular detection over a range of concentrations. Benzenethiol (BT) was immobilized on the gold surface by dipping the substrate into dilute BT solutions (20 mM, 2 mM, 200 μM and 20 μM) in ethanol. After 6 hours of incubation in the BT solution, Raman signals from the nanoforest arrays were acquired using a simple fiber-type Raman system (QE65000-RAMAN-KIT, Ocean Optics Inc.) under the following conditions: 785 nm laser, 50 mW, 5 s simultaneous excitation and acquisition.[23] For comparison, a 50 nm gold film-coated silicon wafer was used as a reference. As shown in Fig. S5†, BT molecules adsorbed onto the nanoforest were detected at concentrations as low as 20 μM.

We have proposed the preparation of gold nanoforests, which are hybrid plasmonic structures with tunable plasmonic extinctions in the visible range. The vertical and lateral feature sizes were controlled by varying the fabrication conditions to precisely tune the plasmonic properties of the nanoforests. Vivid reflection colors from the plasmonic substrates were obtained, and the reflected colors depended on the shape of the nanostructure and their extinction spectra. The plasmonic properties were highly sensitive to changes in the RI, and the reflected colors of the plasmonic substrates could be varied by applying solvents with different RIs. The sensitivity to the surrounding RI depended strongly on the morphology of the nanostructures. Gold nanoforests are attractive for use in applications in which strong uniform local field enhancements are required, as in SERS or plasmonic nano-imaging. Nanoforest substrates, which feature uniformly ordered hybrid plasmonic structures, could be prepared *via* inexpensive robust methods and show potential for use in plasmonic detection devices.

Acknowledgements

This work was supported by a grant from the Creative Research Initiative Program of the MEST/KRF for "Complementary Hybridization of Optical and Fluidic Devices for Integrated Opto-fluidic Systems." The authors also appreciated partial support from the Brain Korea 21 Program.

Notes and references

‡ *Fabrication of a hybrid mask for deposition*: tree-shaped deposition mask arrays were fabricated *via* colloidal lithography. A PS (Sigma-Aldrich, M_w ~212 000) thin film was coated onto a silicon wafer by spin-casting a PS–toluene solution at various concentrations and spin speeds (0.5–2.0 wt%, 2000 or 4000 rpm). The intrinsic hydrophobic character of PS was changed to hydrophilic by modifying the PS surface *via* exposure of the PS film to mild O_2 plasma treatment for 1 min. Monodispersed silica particles 200 nm in diameter were spin-cast (7 wt% silica ethanolic suspension, at 1500 rpm) onto the O_2 plasma-treated PS surface, resulting in a self-assembled hexagonal array. The use of high-quality silica particles is important in the subsequent lithographic processes because the silica assembly acts as a mask. Monodispersed silica particles were synthesized by a seeded-growth procedure, which was a modification of the conventional Stöber–Fink–Bohn method for preparing silica colloids with precisely controlled size. The size of the silica spheres was reduced by reactive ion etching (RIE, Vacuum Science Inc.) with CF_4 gas (80 sccm) under an RF power of 80 W, and further etching of the PS films could be accomplished with O_2 gas under the same conditions. *Optical characterization*: the surface morphologies of the prepared nanostructures were imaged by field emission scanning electron microscopy (FE-SEM, Philips-XL20SFEG). The extinction properties of the nanoforest structures were characterized by measuring the reflection spectrum in the visible range. An optical microscope (Eclipse L150, Nikon) equipped with a spectrometer (USB4000, Ocean Optics) was used to illuminate the substrates with white light through a 10× objective lens and the reflected light from the substrates was collected. The reflected colors from the samples were characterized by imaging the substrates under 200× magnification using the same optical microscopy system. For our system, the white light source for illumination was a halogen lamp which was usually used to obtain micro-images through the optical microscopy technique. Under normal illumination (incident angle was 90° to the substrate surface), reflected colors from substrates were recorded through an optical microscope equipped with a CCD camera. Reflectance spectra of one plasmonic substrate were measured at various angles to confirm that the reflected colors from the samples were due to plasmonic rather than photonic effects (see Fig. S6†). Also, to clarify the reflected images in Fig. 2, 3 and S3†, the original OM images were reproduced in Fig. S7†.

1 J. N. Anker, W. P. Hall, O. Lyandres, N. C. Shah, J. Zhao and R. P. Van Duyne, *Nat. Mater.*, 2008, **7**, 442.
2 S. Lal, S. Link and N. J. Halas, *Nat. Photonics*, 2007, **1**, 641.
3 M. E. Stewart, C. R. Anderton, L. B. Thompson, J. Maria, S. K. Gray, J. A. Rogers and R. G. Nuzzo, *Chem. Rev.*, 2008, **108**, 494.
4 H. C. Jeon, C. J. Heo, S. Y. Lee, S. G. Park and S. M. Yang, *J. Mater. Chem.*, 2012, **22**, 4603.
5 J. Zhao, A. Das, X. Y. Zhang, G. C. Schatz, S. G. Sligar and R. P. Van Duyne, *J. Am. Chem. Soc.*, 2006, **128**, 11004.
6 C. J. Heo, S. H. Kim, S. G. Jang, S. Y. Lee and S. M. Yang, *Adv. Mater.*, 2009, **21**, 1726.
7 M. Hu, J. Chen, Z.-Y. Li, L. Au, G. V. Hartland, X. Li, M. Marquez and Y. Xia, *Chem. Soc. Rev.*, 2006, **35**, 1084.
8 Y. Choi, S. Hong and L. P. Lee, *Nano Lett.*, 2009, **9**, 3726.
9 L. A. Dick, A. D. McFarland, C. L. Haynes and R. P. Van Duyne, *J. Phys. Chem. B*, 2002, **106**, 853.
10 S. G. Jang, D. G. Choi, C. J. Heo, S. Y. Lee and S. M. Yang, *Adv. Mater.*, 2008, **20**, 4862.
11 G. L. Liu, Y. T. Long, Y. Choi, T. Kang and L. P. Lee, *Nat. Methods*, 2007, **4**, 1015.
12 Y. Choi, Y. Park, T. Kang and L. P. Lee, *Nat. Nanotechnol.*, 2009, **4**, 742.
13 S. R. Forrest, *Nature*, 2004, **428**, 911.
14 M. E. Stewart, N. H. Mack, V. Malyarchuk, J. A. N. T. Soares, T. W. Lee, S. K. Gray, R. G. Nuzzo and J. A. Rogers, *Proc. Natl. Acad. Sci. U. S. A.*, 2006, **103**, 17143.
15 J. Henzie, M. H. Lee and T. W. Odom, *Nat. Nanotechnol.*, 2007, **2**, 549.
16 J. Theiss, P. Pavaskar, P. M. Echternach, R. E. Muller and S. B. Cronin, *Nano Lett.*, 2010, **10**, 2749.
17 S. Lee, J. Shin, Y. H. Lee, S. Fan and J. K. Park, *Nano Lett.*, 2010, **10**, 296.
18 E. Prodan, C. Radloff, N. J. Halas and P. Nordlander, *Science*, 2003, **302**, 419.
19 S. M. Yang, S. G. Jang, D. G. Choi, S. Kim and H. K. Yu, *Small*, 2006, **2**, 458.
20 H. K. Choi, S. H. Im and O. O. Park, *Langmuir*, 2009, **25**, 12011.
21 S. Berciaud, L. Cognet, P. Tamarat and B. Lounis, *Nano Lett.*, 2005, **5**, 515.
22 S. Y. Lee, S. Kim, S. G. Jang, C. J. Heo, J. W. Shim and S. M. Yang, *Anal. Chem.*, 2011, **83**, 9174.
23 H. Hwang, S. H. Kim and S. M. Yang, *Lab Chip*, 2011, **11**, 87.